Reetuparna Ghosh*, Bioletty Lawriniang, Sylvia Badwar, Santhi Sheela Yerraguntla, Haladhara Naik, Bhushankumar J. Patil, Yeshwant Naik, Saraswatula Venkata Suryanarayana, Betylda Jyrwa and Srinivasan Ganesan

Measurement and uncertainty propagation of the (γ,n) reaction cross-section of ^{58}Ni and ^{59}Co at 15 MeV bremsstrahlung

https://doi.org/10.1515/ract-2017-2855
Received July 21, 2017; accepted November 2, 2017; published online December 21, 2017

Abstract: Activation cross-section of photon-induced reaction on structural materials ^{58}Ni and ^{59}Co was measured at the bremsstrahlung endpoint energy 15 MeV from an S band electron linac. The uncertainties in the (γ,n) reaction cross-section of both ^{58}Ni and ^{59}Co were estimated by using the concept of covariance analysis. The cross-section of ^{58}Ni(γ,n)^{57}Ni reaction in the present work is slightly lower than the previous experimental data and the TENDL-2015 data. The cross-section of ^{59}Co(γ,n)^{58}Co reaction has been measured for the first time. However, the present experimental data of ^{59}Co(γ,n)^{58}Co reaction is very low in comparison to the TENDL-2015 and JENDL/PD-2004 data.

Keywords: Photonuclear reaction cross-section, bremsstrahlung, coincidence summing, ratio measurement technique, covariance analysis.

***Corresponding author: Reetuparna Ghosh,** Department of Physics, North Eastern Hill University, Shillong 793022, Meghalaya, India, E-mail: reetuparna.ghosh@gmail.com
Bioletty Lawriniang, Sylvia Badwar and Betylda Jyrwa: Department of Physics, North Eastern Hill University, Shillong 793022, Meghalaya, India
Santhi Sheela Yerraguntla: Department of Statistics, Manipal University, Manipal 576104, India
Haladhara Naik: Radiochemistry Division, Bhabha Atomic Research Centre, Mumbai 400085, India
Bhushankumar J. Patil: Department of Physics, Abasaheb Garware College, Karve Road, Pune 411004, India
Yeshwant Naik: Product Development Division, Bhabha Atomic Research Centre, Mumbai 400085, India
Saraswatula Venkata Suryanarayana: Nuclear Physics Division, Bhabha Atomic Research Centre, Mumbai 400085, India
Srinivasan Ganesan: Raja Ramana Fellow of DAE, HBNI, Bhabha Atomic Research Centre, Mumbai 400085, India

1 Introduction

Photonuclear reactions have a great importance in many fields as they serve as microscope for the structure and dynamics of atomic nucleus. Photonuclear reaction data play a prominent role in radiation shielding design and radiation transport analysis, particularly above the neutron separation energy (~8 MeV), calculation of absorbed dose in human body during radiation therapy and in astrophysical nucleosynthesis. They are also important for the development and understanding of physics and technology of fission as well as fusion reactors, for nuclear waste transmutation and for activation analysis, safeguards and inspection technologies. Photonuclear data also find application in reactor-in-core-dosimetry, radiation damage in reactor structural materials, fast reactor design studies and in design of accelerator driven sub-critical systems [1, 2]. Thus, photonuclear reaction cross-section data are required for a wide variety of applications. In this context, the photonuclear reaction cross-section measurement of ^{58}Ni and ^{59}Co has been measured corresponding to the bremsstrahlung spectrum of 15 MeV electrons. The photonuclear reaction cross-sections of ^{58}Ni and ^{59}Co are significant from the nuclear reactor point of view as Ni and Co are important structural materials [1].

The uncertainty in the present work has been generated using covariance analysis. It was an initiative taken by Department of Atomic Energy, Bhabha Atomic Research Centre, Mumbai to evolve a program on nuclear data covariance in India [3]. As per the program, the covariance information should be generated in all Indian nuclear physics experiments as a fundamental approach. Covariance analysis has been profoundly used to generate the uncertainty information in the case of evaluated nuclear data of neutron-induced reactions in files such as TENDL-2015. Though the experimental works reported in EXFOR show that even in the case of neutron induced reactions only a handful of experimenters have performed a detailed covariance analysis, in the case of

photonuclear reactions even the evaluated files rarely provide covariance information. Also it was found [4] that barely any experimenter has performed a detailed covariance analysis. This paper provides covariance analysis for the gamma induced reaction for the first time. Covariance analysis has been performed in the present work as proper specification of uncertainties is complete only with the covariance information.

2 Experimental details

The experiment was performed by using bremsstrahlung photon with endpoint energy of 15 MeV, in the electron linac of SAMEER, at Navi-Mumbai, India. The 15 MeV electron linac is a π/2 S band standing wave side coupled compact electron linac, with the flange to flange length of 1.2 m. A 5.5 MW Klystron source, at 117–878 W, was used as an RF source [5]. The linac tube was successfully operated at a peak current of 65 mA with 6 μs pulse width and pulse repetition rate of 20–150 Hz. The bremsstrahlung was produced by impinging an electron beam of energy 15 MeV on a water cooled circular tungsten metal foil. The diameter of the tungsten foil was 6 mm and the thickness was 4 mm. A target assembly of Co, Au and Ni was made for the irradiation. The ^{197}Au foil with purity 99.99 % of size 0.4 cm × 0.4 cm, weighing 0.0490 g was used to normalize the cross-section of the targets. On the other hand a circular ^{59}Co foil (99.99 % purity), with a diameter of 0.55 cm, weighing 0.2282 g and a ^{nat}Ni foil of size 0.4 × 0.4 cm^2 weighing 0.0134 g were used as the targets. All the samples were individually wrapped with 0.025 mm thick pure aluminium to avoid contamination during the irradiation process. The target assembly was irradiated for 5 min. The irradiated targets were cooled for 1.97 h and were separately mounted on Perspex plates for counting.

3 Data analysis

3.1 Calibration and calculation of detector efficiency

The γ-ray activities of the irradiated samples were measured by using a 105 cm^3 high purity germanium detector (HPGe) coupled to a PC-based 4K multi-channel analyzer. The efficiency of the HPGe detector used was 20 % relative to 3″ diameter × 3″ length NaI(Tl) detector and the resolution was 1.8 keV (FWHM) at 1332.5 keV. The energy and efficiency calibration of the detector system was performed by counting the γ-rays of the standard ^{152}Eu point-source keeping it at a distance of 1 cm from the end cap of the detector. The standard equation for the full-energy peak efficiency (ε) of detector, for a point source was used to obtain the efficiency of the detector,

$$\varepsilon = \frac{CK_c}{A_0 e^{-\lambda T} I_\gamma \Delta t} \quad (1)$$

where, C represents the net peak area measured in time Δt, K_c is the correction factor for the coincidence-summing effect [6], I_γ is the intensity of the γ- transition, A_0 is the source strength at the time of standardization, and T is the time elapsed between standardization and calibration, λ is the decay constant related to the half-life ($T_{1/2}$) of the source by,

$$\lambda = \frac{\ln 2}{T_{1/2}} \quad (2)$$

As the point source was placed at a close distance to the detector, it introduces coincidence summing effect, which was corrected by introducing the factor, K_c. Since, the detector was calibrated using point source and the samples were of finite size, the efficiency obtained has to be transferred to the full-energy peak efficiency for the samples. The coincidence summing correction and the efficiency transfer for the detector were performed using the EFFTRAN code [7] based on Monte-Carlo simulations. The comparison among the efficiency of the point source with and without coincidence summing effect and also the efficiency of the sample after accomplishing the efficiency transfer are presented in Figure 1.

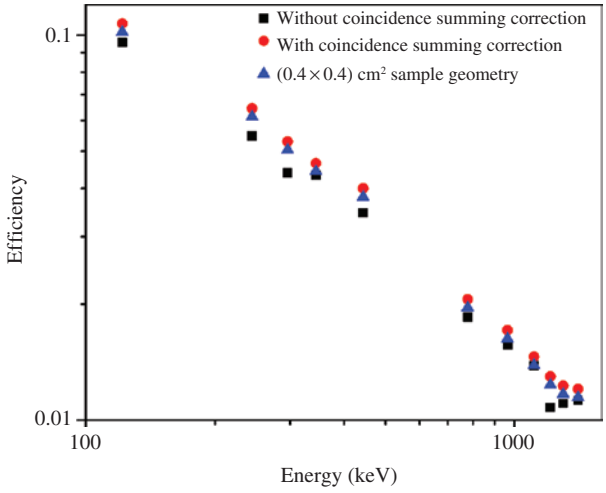

Figure 1: Detector efficiency as a function of γ-energy for point source without and with summing correction, and for sample after transferring the efficiency.

3.2 Uncertainty propagation in efficiency calculation

The energy and efficiency calibration of the HPGe detector was performed using 11 γ-lines of ^{152}Eu point source. The uncertainty in the efficiency, calculated using equation (1), was introduced by the uncertainties of the attributes C, I_γ, A_0 and λ. According to the law of uncertainty propagation under linear approximation applicable to small uncertainties [8, 9], the uncertainty in the efficiency (ε_i) due to the i-th γ-line can be propagated as,

$$(\Delta\varepsilon_i)^2 = \sum_{r=1}^{4}\left(\frac{\partial\varepsilon_i}{\partial q_{ri}}\Delta q_{ri}\right)^2,\ 1\le i\le 11 \tag{3}$$

where, q represents the attributes, r denotes the number of attributes. The partial uncertainty due to each attribute, except λ, was obtained as,

$$\frac{\partial\varepsilon_i}{\partial q_i}\Delta q_i = \frac{\Delta q_i}{q_i}\varepsilon_i \tag{4}$$

From equation (1), the partial uncertainty due to the uncertainty in the decay constant was obtained as,

$$\frac{\partial\varepsilon_i}{\partial\lambda}\Delta\lambda = t\varepsilon_i\Delta\lambda \tag{5}$$

where, the uncertainty in the decay constant was obtained from the uncertainty in the half-life as,

$$\Delta\lambda = \frac{\ln 2\Delta T_{1/2}}{T_{1/2}^{\ 2}} \tag{6}$$

The decay data for ^{152}Eu, like $T_{1/2}$ and I_γ, were taken from the ENSDF evaluation [10] retrieved through the web based interface NUDAT 2.7β [11]. The characteristic γ-ray energies of ^{152}Eu as well as the corresponding gamma intensities and their uncertainties used in the present work have been listed in Table 1 [11].

Similarly, the uncertainty in (ε_j) due to the j-th γ-line is,

$$(\Delta\varepsilon_j)^2 = \sum_{r=1}^{4}\left(\frac{\partial\varepsilon_j}{\partial q_{rj}}\Delta q_{rj}\right)^2,\ 1\le j\le 11 \tag{7}$$

These four attributes are measured independently so no correlation prevails among the attributes, i.e. the measurement of C is not affected by the other attributes like $T_{1/2}$, I_γ, or A_0. However, there exists correlation within the attributes. For instance, the attribute A_0 is common for all the γ-lines and so there exists correlation within the attribute A_0. Hence using this information on partial uncertainties and their correlation the covariance matrix ($\boldsymbol{V_\varepsilon}$) for the efficiency of the detector can be constructed. The elements of this covariance matrix can be calculated as,

$$V_{\varepsilon ij} = \sum_{r=1}^{4}\left(\frac{\partial\varepsilon_i}{\partial q_{ri}}\Delta q_{ri}\right)\mathrm{cor}\,(q_{ri},q_{rj})\left(\frac{\partial\varepsilon_j}{\partial q_{rj}}\Delta q_{rj}\right) \tag{8}$$

where, cor(q_{ri},q_{rj}) is the correlation coefficient between q_{ri} and q_{rj} [12]. The micro-correlation matrix for C and I_γ can be represented as,

$$\mathrm{cor}\,(q_{ri},q_{rj}) = \delta_{ij} \tag{9}$$

where, δ_{ij} is the Kronecker-delta function. However, for A_0 and λ the micro-correlation matrix is given by,

$$\mathrm{cor}\,(q_{ri},q_{rj}) = 1 \tag{10}$$

This is because the observations of A_0 and λ are fully correlated, so the micro-correlation matrix for each of these attributes will be a matrix J of order 11 with all the entries equal to one.

The characteristic γ-rays for our samples are, however, different than those of the calibration source. In order to obtain the efficiencies of the required characteristic γ-rays, an appropriate model for interpolation was chosen with the help of the following empirical formula,

$$\ln\varepsilon_i = \sum_{m=1}^{4} p_m(\ln E_i)^{m-1} \tag{11}$$

where, E_i is the energy of the γ-lines and p_m is the fitting parameter. Equation (11) can be depicted in matrix form as,

$$\boldsymbol{Z\approx AP} \tag{12}$$

Table 1: Characteristic γ-ray energies and their gamma abundances of ^{152}Eu.

Gamma energy (keV)	Gamma abundance (%)
121.78	28.53 ± 0.16
244.7	7.55 ± 0.04
295.94	0.440 ± 0.004
344.28	26.59 ± 0.20
411.12	2.237 ± 0.013
778.9	12.93 ± 0.08
964.06	14.51 ± 0.07
1112.1	13.67 ± 0.08
1212.9	1.415 ± 0.008
1299.1	1.633 ± 0.011
1408.013	20.87 ± 0.09

where, the elements of the column matrix $\boldsymbol{Z}$ is given by $\ln\varepsilon_i$, $\boldsymbol{P}$ is the column matrix with elements p_m and the design matrix $\boldsymbol{A}$ of order 11× m with elements,

$$A_{i\,m} = (\ln E_i)^{m-1} \tag{13}$$

The best model for the interpolation was chosen based on the minimum Chi-square (χ^2) statistics, which is given by,

$$\chi^2 = (\boldsymbol{Z} - \boldsymbol{AP})^T \boldsymbol{V}_Z^{-1} (\boldsymbol{Z} - \boldsymbol{AP}) \tag{14}$$

where, $(\boldsymbol{Z} - \boldsymbol{AP})^T$ is the transpose of the matrix of $(\boldsymbol{Z} - \boldsymbol{AP})$ and $\boldsymbol{V}_Z^{-1}$ is the inverse of matrix of $\boldsymbol{V}_Z$. The elements of the matrix $\boldsymbol{V}_Z$ were obtained using the law of uncertainty propagation between $\boldsymbol{z}_i$ and $\boldsymbol{\varepsilon}_i$ as,

$$(\boldsymbol{V}_Z)_{ij} = \frac{(\boldsymbol{V}_\varepsilon)_{ij}}{\boldsymbol{\varepsilon}_i \boldsymbol{\varepsilon}_j} \tag{15}$$

By using the method of least squares, the best solution $\boldsymbol{P}$ was obtained by,

$$\boldsymbol{P} = \boldsymbol{V}_p (\boldsymbol{A}^T \boldsymbol{V}_Z^{-1} \boldsymbol{Z}) \tag{16}$$

where, the covariance matrix for the solution parameters ($\boldsymbol{V}_p$) is given by,

$$\boldsymbol{V}_p = (\boldsymbol{A}^T \boldsymbol{V}_Z^{-1} \boldsymbol{Z})^{-1} \tag{17}$$

The goodness of the fit thus obtained is tested by obtaining $\chi^2/(n-m) \sim 1$ where n represents the number of γ-ray energies of ^{152}Eu considered in the present work. Thus, after obtaining the matrix $\boldsymbol{P}$, the required efficiencies for the characteristic γ-rays of the samples Au, Ni and Co are calculated using equations (11–13). The minimum χ^2 in this case was obtained for $m = 4$, which is presented in Table 2 along with the corresponding p_m values and the correlation matrix. The interpolated detector efficiencies of the radionuclides in the present work are reported in Table 3 along with their covariance and correlation matrix. The interpolated efficiencies along with the measured ones are shown in Figure 2.

Table 2: Fitting parameters and minimum χ^2 value for fitting model $m = 4$.

Parameter	Value	Correlation coefficient (%)			
p_1	−4.166 ± 0.0124	100			
p_2	−0.934 ± 0.014	−17	100		
p_3	0.122 ± 0.023	−26	87	100	
p_4	0.067 ± 0.008	−26	76	98	100

The goodness of the fit is 1.486.

Table 3: Detector efficiencies for the reaction products and the covariance matrix for the efficiencies and the corresponding correlation matrix.

Radionuclide	E_γ (keV)	Efficiency × 10^{-2} (absolute)	Correlation matrix (%)		
^{196}Au	355.73	4.310 ± 0.054	100		
^{58}Co	810.76	1.896 ± 0.024	87	100	
^{57}Ni	1377.63	1.167 ± 0.015	78	75	100

3.3 Cross-section calculation

Ratio measurement was used to obtain the photonuclear reaction cross-section of ^{59}Co and ^{58}Ni. In this method the cross-section of the target was calculated relative to the cross-section of the monitor reaction ^{197}Au(γ,n)^{196}Au. The photonuclear cross-section (σ_s) for each Co and Ni was calculated as,

$$\sigma_s = \langle \sigma_{\mathrm{Au}} \rangle \frac{C_s N_{\mathrm{Au}} I_{\gamma \mathrm{Au}} \varepsilon_{\gamma \mathrm{Au}} (1 - e^{-\lambda_{\mathrm{Au}} T_i}) e^{-\lambda_{\mathrm{Au}} T_c} (1 - e^{-\lambda_{\mathrm{Au}} t})}{C_{\mathrm{Au}} N_s I_{\gamma s} \varepsilon_{\gamma s} (1 - e^{-\lambda_s T_i}) e^{-\lambda_s T_c} (1 - e^{-\lambda_s t}) R_\varphi} \times \frac{\lambda_s}{\lambda_{\mathrm{Au}}} \tag{18}$$

where, C gives the total counts of the sample, $\langle \sigma_{\mathrm{Au}} \rangle$ is the flux-weighted average cross-section of the ^{197}Au(γ,n)^{196}Au reaction, I_γ is the branching intensity of the activation product, N represents the number of the target atoms calculated from the weight of the target material, ε is the detector efficiency, T_i, T_c and t are the irradiation time, cooling time and counting time of the samples, respectively and λ is the decay constant for the respective nuclide. The term R_φ is the flux ratio used to normalize the cross-sections as the targets and the monitor have different threshold

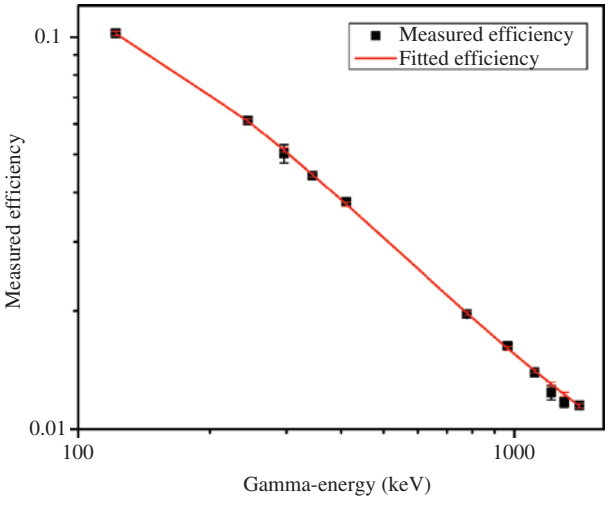

Figure 2: Comparison between the measured efficiency and fitted efficiency.

Table 4: Reaction thresholds of the reactions [13] and the flux ratio of the ^{59}Co(γ,n)^{58}Co and ^{58}Ni(γ,n)^{57}Ni.

Reaction	Threshold energy (MeV)	Flux-ratio
^{197}Au(γ,n)^{196}Au	8.073	
^{59}Co(γ,n)^{58}Co	10.455	4.609×10^{-1}
^{58}Ni(γ,n)^{57}Ni	12.218	2.021×10^{-1}

energy, which are presented in Table 4. The threshold energies of the reactions were calculated using Q-tool [14]. The flux ratio is calculated by [13],

$$R_{\varphi} = \frac{\int_{E_{\text{th-s}}}^{E_{\gamma\max}} \varphi(E)}{\int_{E_{\text{th-m}}}^{E_{\gamma\max}} \varphi(E)dE} \tag{19}$$

where, $E_{\text{th-m}}$ and $E_{\text{th-s}}$ represent the threshold energies of the monitor and sample, respectively. The photon flux (φ) was taken from the bremsstrahlung spectrum (Figure 3). As the measurement of bremsstrahlung fluence spectrum is a difficult task, we calculated it using FLUKA 2011.2c.6 [15–18] by simulating the photon production under the geometry of our experimental setup. The 15 MeV electron beam was allowed to fall on a Tungsten target and the bremsstrahlung spectrum was estimated at a distance of 24.5 cm from the tungsten target. The bremsstrahlung spectrum, thus, obtained is shown in Figure 3. The flux-ratio for Co and Ni are given in Table 4. For simplicity, equation (18) is rewritten as

$$\sigma_s = \langle\sigma_{\text{Au}}\rangle \frac{C_s N_{\text{Au}} I_{\gamma\text{Au}} \varepsilon_{\gamma\text{Au}} f_{\text{Au}}}{C_{\text{Au}} N_s I_{\gamma s} \varepsilon_{\gamma s} f_s R_{\varphi}} \tag{20}$$

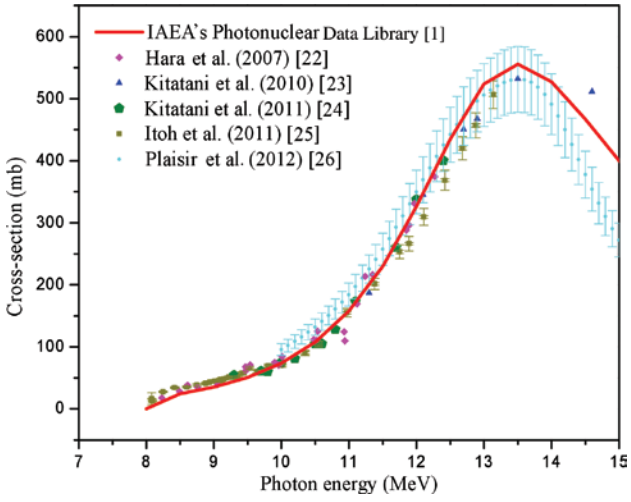

Figure 3: Plot of experimental and evaluated data from the IAEA Photonuclear Data Library of ^{197}Au(γ,n)^{196}Au reaction as a function of photon energy.

$$\text{where, } f = \frac{(1-e^{-\lambda T_i})e^{-\lambda T_c}(1-e^{-\lambda t})}{\lambda} \tag{21}$$

The photo-peak counts of the different γ-rays of the interested reaction product of interest were obtained by subtracting the Compton background from the gross peak area. The γ-ray energies and the nuclear spectroscopic data such as the half-lives and branching intensity were taken from the ENSDF evaluation [19–21] retrieved through the web interface NUDAT 2.7β [11] and given in Table 5.

In equation (3), the number atoms in a target material was calculated as,

$$N = \frac{N_A \times W \times a}{A_v} \tag{22}$$

where, N_A is the Avogadro's number, which was not considered in equation (18) as it gets canceled out in ratio method. The weight of the sample is represented by W, A_V is the atomic weight of the element and a denotes the isotopic abundance of the particular target isotope. Thus, equation (18) takes the following form, which was used for the calculation in the present work,

$$\sigma_s = \langle\sigma_{\text{Au}}\rangle \frac{C_s W_{\text{Au}} a_{\text{Au}} A_{VS} I_{\gamma\text{Au}} \varepsilon_{\gamma\text{Au}} f_{\text{Au}}}{C_{\text{Au}} W_s a_s A_{V\text{Au}} I_{\gamma s} \varepsilon_{\gamma s} f_s R_{\varphi}} \tag{23}$$

Since the accelerated electrons after hitting the tungsten foil generate a bremsstrahlung of photons at 15 MeV, the cross-section of ^{197}Au(γ,n)^{196}Au reaction provided by the IAEA Photonuclear Data Library [1] for mono-energetic photon source was converted to flux-weighted average cross-section. The comparison between the cross-section of the ^{197}Au(γ,n) ^{196}Au reaction from literature [22–26] and the IAEA's Photonuclear Data Library [1] is shown in Figure 3. The flux weighted average values of the cross-section of ^{196}Au from energy threshold to the endpoint bremsstrahlung energy was calculated using the following relation [13],

$$\langle\sigma_{\text{Au}}\rangle = \frac{\int_{E_{\text{th-m}}}^{E_{\gamma\max}} \varphi(E)\sigma(E)dE}{\int_{E_{\text{th-m}}}^{E_{\gamma\max}} \varphi(E)dE} \tag{24}$$

where, $\varphi(E)$ is the photon flux for the ^{197}Au(γ,n)^{196}Au reaction. The photon flux (φ) was taken from the bremsstrahlung spectrum, shown in Figure 4 and the cross-section values $\sigma(E)$ were taken from the IAEA Photonuclear Data Library maintained by IAEA [1].

Table 5: Nuclear spectroscopic data of the radionuclides from Ref. [12].

Reaction	Nuclides	Half-life	Decay mode %	γ-ray energy E_γ (keV)	γ-ray intensity I_γ (%)
^{197}Au(γ,n)	^{196}Au	6.1669 ± 0.0006 days	EC (93.0) β$^-$ (7.0)	355.73 ± 0.05	87 ± 3
^{59}Co(γ,n)	^{58}Co	70.86 ± 0.06 days	EC (100)	810.7593 ± 0.0020	99.450 ± 0.01
^{58}Ni(γ,n)	^{57}Ni	35.60 ± 0.06 h	EC (100)	1377.63 ± 0.003	81.7 ± 2.4

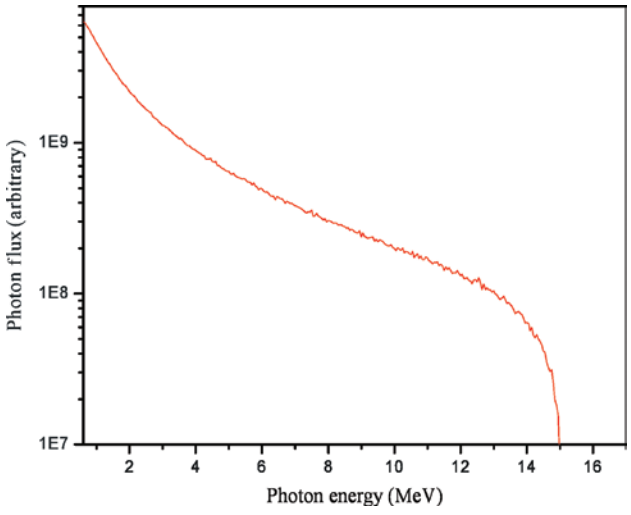

Figure 4: Bremsstrahlung spectrum with end point energy of 15 MeV calculated using FLUKA 2011.2c.6.

3.4 Uncertainty propagation in cross-section measurement

The attributes that contribute to the uncertainty in the cross-section are C, W, A_v, a, I_γ, f and ε of the reaction target nuclide (^{59}Ni or ^{58}Co) and the monitor target nuclide (^{197}Au), namely there are $7\times2=14$ attributes in determination of a reaction cross-section. Due to lack of uncertainty information for both the quantities R_φ and $<\sigma_{Au}>$, they have not been considered in the uncertainty analysis. Also, the uncertainties in weight of the sample and atomic weight of the element are too small to contribute to the uncertainty propagation and are not considered. The uncertainty in the cross-section of each of the target, can be calculated as,

$$\left(\frac{\Delta\sigma_s}{\sigma_s}\right)^2=\sum_{r=1}^{9}\left(\frac{\Delta q_{rs}}{q_{rs}}\right)^2+2\left(\frac{\Delta\varepsilon_s}{\varepsilon_s}\right)\mathrm{cor}(\varepsilon_s,\varepsilon_{Au})\left(\frac{\Delta\varepsilon_{Au}}{\varepsilon_{Au}}\right) \quad (25)$$

where, q represents the attributes and s is used for the targets, ^{58}Ni and ^{59}Co. Equation (25) is explicitly described in the Appendix. The terms T_i, T_c and t in equation (20) are considered to have negligible uncertainty and were not considered in the uncertainty propagation of f. Thus the only term contributing to the uncertainty in f is λ. Since, λ is connected to σ exponentially; the partial uncertainty in f was calculated by [27],

$$\left(\frac{\Delta f}{f}\right)^2=s_{f\lambda}{}^2\left(\frac{\Delta\lambda}{\lambda}\right)^2 \quad (26)$$

where, the sensitivity coefficient $s_{f\lambda}$ was calculated as,

$$s_{f\lambda}=\frac{\lambda}{f}\frac{\partial f}{\partial\lambda}=\left(\frac{\lambda T_i e^{-\lambda T_i}}{1-e^{-\lambda T_i}}-\lambda T_C+\frac{\lambda t e^{-\lambda t}}{1-e^{-\lambda t}}-1\right) \quad (27)$$

The uncertainty in λ was propagated as done in the earlier section, equation (6).

The fractional covariance between the cross-section of ^{58}Co and ^{57}Ni is be obtained as,

$$\mathrm{cov}(\sigma_{Co},\sigma_{Ni})=\sum_{r=1}^{4}\left(\frac{\Delta q_{rAu}}{q_{rAu}}\right)^2+\left(\frac{\Delta\varepsilon_{Co}}{\varepsilon_{Co}}\right)\mathrm{cor}(\varepsilon_{Co},\varepsilon_{Ni})\left(\frac{\Delta\varepsilon_{Ni}}{\varepsilon_{Ni}}\right)-\left(\frac{\Delta\varepsilon_{Co}}{\varepsilon_{Co}}\right)\mathrm{cor}(\varepsilon_{Co},\varepsilon_{Au})\left(\frac{\Delta\varepsilon_{Au}}{\varepsilon_{Au}}\right)-\left(\frac{\Delta\varepsilon_{Ni}}{\varepsilon_{Ni}}\right)\mathrm{cor}(\varepsilon_{Ni},\varepsilon_{Au})\left(\frac{\Delta\varepsilon_{Au}}{\varepsilon_{Au}}\right) \quad (28)$$

In equation (28), r represents the attributes C, I_γ, ε and f for Au. In the present work, there is correlation among the efficiency of the detector for the targets and the monitor (ε_s and ε_{Au}) and this correlation is developed due to the model used for interpolation to obtain the efficiencies for the targets and the monitor. Hence, except for the efficiency, the observation between any two attributes, like (C, W) or (C, A_v) and so on is independent of each other. The fractional uncertainty in all the attributes, except efficiency along with their correlation is presented in Table 6. The fractional uncertainty in the efficiency of the detector for the characteristic γ-rays of ^{57}Ni, ^{58}Co and ^{196}Au can be obtained from Table 3 and the correlation coefficients are presented in Table 3. Using all the fractional uncertainty and correlation information from Table 3 and Table 6 in equation (23), the required covariance matrix in cross-section between ^{58}Ni and ^{59}Co is obtained. Thus, the final covariance matrix can be obtained using equations (25) and (28) [28, 29]. The

Table 6: Fractional uncertainties (%) in various attributes in obtaining the cross-section of ^{59}Co(γ,n)^{58}Co and ^{58}Ni(γ,n)^{57}Ni reactions relative to the cross-section of ^{197}Au (γ,n)^{196}Au monitor reaction.

s	C_s	C_{Au}	a_s	$I_{\gamma s}$	$I_{\gamma Au}$	f_s	f_{Au}
1 (Co)	2.38	1.164		0.010	3.448	0.833	0.010
2 (Ni)	4.466		0.028	2.938		0.151	
Corr	0	1	0	0	1	0	1

Correlation within the attribute are represented by Corr.

Table 7: Uncertainties in the cross-sections measurement for the ^{59}Co(γ,n)^{58}Co and ^{58}Ni(γ,n)^{57}Ni reactions relative to the cross-section of ^{197}Au (γ,n) ^{196}Au monitor reaction.

Radionuclide	E_γ (keV)	Cross-section (mb)	Correlation coefficients (%)	
^{58}Co	810.76	3.170 ± 0.142	100	
^{57}Ni	1377.63	11.519 ± 0.751	46	100

correlation matrix between the two reaction cross-sections of interest and the uncertainty in the cross-section values thus obtained are presented in Table 7.

4 Discussion

The bremsstrahlung spectrum averaged ^{59}Co(γ,n)^{58}Co and ^{58}Ni(γ,n)^{57}Ni cross-sections at the end point energy of 15 MeV are listed in Table 7 along with their uncertainties and correlation coefficients. There are no bremsstrahlung averaged cross-sections of the reactions of interest in EXFOR. The energy dependent cross-sections in TENDL-2015 [30, 31], JENDL/PD-2004 [32] and the IAEA's Photonuclear Data Library [1] have been converted to the bremsstrahlung averaged cross-section with end point energy of 15 MeV by using equation (24) and compared with our result in Table 8. The energy dependent cross-sections from literature [33–40] and various libraries [1, 30, 32] for

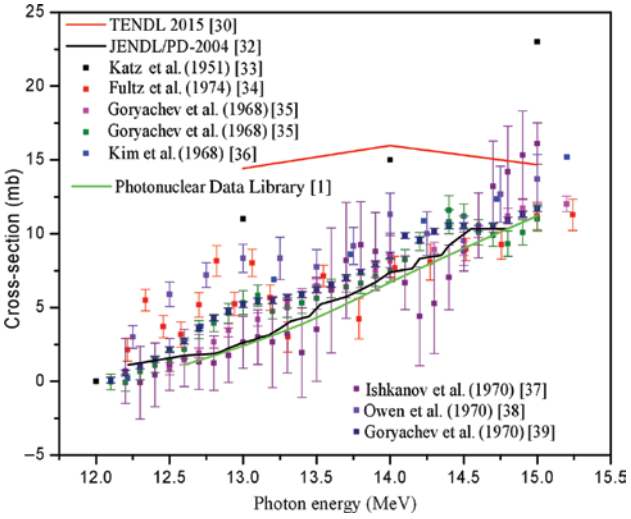

Figure 5: Plot of literature, TENDL and JENDL/PD-2004 data of ^{58}Ni(γ,n)^{57}Ni reaction as a function of photon energy.

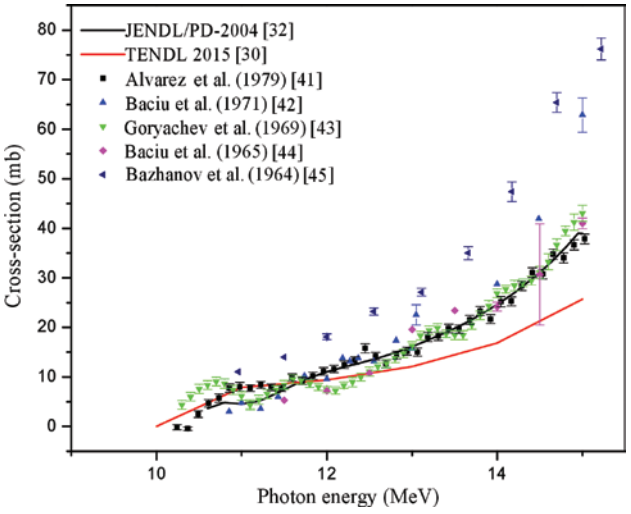

Figure 6: Plot of literature, TENDL 2015 and JENDL/PD-2004 data of ^{59}Co(γ,n)^{58}Co reaction as a function of photon energy.

^{58}Ni(γ,n)^{57}Ni reaction are presented in Figure 5. Similarly, the energy dependent cross-sections from literature [41–45] and various libraries [30, 32] for ^{59}Co(γ,n)^{58}Co reaction are presented in Figure 6.

Table 8: The cross-sections of ^{59}Co(γ,n)^{58}Co and ^{58}Ni(γ,n)^{57}Ni reactions at the bremsstrahlung end-point energy of 15 MeV.

Reaction	Energy (MeV)	Cross-section (mb)			
		Experimental	TENDL-2015 [30]	JENDL/PD-2004 [32]	IAEA Photonuclear Data Library [1]
^{59}Co(γ,n)^{58}Co	15	3.170 ± 0.142	10.686	10.820	N/A
^{58}Ni(γ,n)^{57}Ni	15	11.519 ± 0.751	14.992	3.971	3.906

The values corresponding to various libraries have been calculated by folding the energy dependent cross-section in [1, 31, 33] using the bremsstrahlung spectrum of the photon field used in the present experiment (Figure 3).

The cross-section for ^{58}Ni(γ,n)^{57}Ni reaction obtained from the present work is slightly lower than the TENDL-2015 value. However, the obtained cross-section for the ^{58}Ni(γ,n)^{57}Ni reaction in the present case was found to be higher than the data obtained from the IAEA Photonuclear Data Library and JENDL/PD-2004. In case of Co, the (γ,n) reaction cross-section obtained from the present experimental work is lower than the value obtained from both the TENDL-2015 and JENDL/PD-2004 libraries.

The uncertainty analysis in the present work has shown that, though the cross-section of ^{59}Co(γ,n)^{58}Co and ^{58}Ni(γ,n)^{57}Ni reactions were measured independently, there still exists a correlation between both the cross-sections due to the same model and parameters used for interpolation of efficiencies. Also, same parameters adopted for the ^{197}Au(γ,n)^{196}Au reaction (i.e. the parameters listed in Table 6 with "1" as the correlation coefficient) for determination of the cross-sections of the two reactions add to the correlation information between them. Hence, the uncertainty in the cross-section measurement of ^{59}Co(γ,n)^{58}Co and ^{58}Ni(γ,n)^{57}Ni reactions are 4.475 % and 6.516 %, respectively, having correlation of 46 % as presented in Table 7. The covariance between the two reaction cross-sections is 0.049 mb.

Acknowledgement: This work has been carried out as a joint collaboration between Department of Physics, North Eastern Hill University and B.A.R.C, Mumbai. One of the authors (R. Ghosh) is greatly indebted to the crew of Society of Applied Microwave Electronics Engineering and Research (SAMEER), for their help in the irradiation of the samples. The author (R. Ghosh) also acknowledges the support of Board of Research in Nuclear Sciences, Department of Atomic Energy, Mumbai for funding the research project. The author is also grateful to Tim Vidmar, SCK CEN, Belgian Nuclear Research Centre, Boeretang 200, BE-2400 Mol, Belgium, for provoding EFFTRAN code. The authors are highly indebted to Dr. N.Otsuka, Nuclear Data Section, International Atomic Energy Agency, Vienna, Austria for helping with the formulation part of the covariance analysis. The authors also thank Prof. B. Lalremruata of Mizoram University, Aizawl for guidance and suggestion for the present work.

Appendix

Determination of uncertainty in cross-section

The cross-section as given in equation (20) is,

$$\sigma_s = \langle \sigma_{\mathrm{Au}} \rangle \frac{C_s W_{\mathrm{Au}} a_{\mathrm{Au}} A_{VS} I_{\gamma \mathrm{Au}} \varepsilon_{\gamma \mathrm{Au}} f_{\mathrm{Au}}}{C_{\mathrm{Au}} W_s a_s A_{V\mathrm{Au}} I_{\gamma s} \varepsilon_{\gamma s} f_s R_\varphi} \tag{A1}$$

The sources of uncertainty in the cross-section calculation are C, W, a, A_V, I_γ, ε and f related to both the sample and the monitor. However, the uncertainty due to weight of the sample and atomic weight of the element (A_V) are negligible so they are not considered in the uncertainty propagation of σ_s. Also, $<\sigma_{\mathrm{Au}}>$ and R_φ are treated as constants as there is lack of uncertainty information for both these quantities. Hence, σ_s can be treated as a function of C, W, a, A_V, I_γ, ε and f and can be expressed as,

$$\sigma_s = F(C,\ a,\ I_\gamma,\ \varepsilon,\ f) \tag{A2}$$

Except for the ε of the sample and the monitor, there does not exist any correlation within the attributes, i.e. the counts of sample are independent of that of the monitor. In case of the efficiency, ε, attribute, the efficiency of the sample is correlated to that of the monitor, due to model used to obtain the efficiencies. Thus the uncertainty in σ_s can be propagated as,

$$\begin{aligned}\left(\frac{\Delta\sigma_s}{\sigma_s}\right)^2 = &\left(\frac{\Delta C_s}{C_s}\right)^2 + \left(\frac{\Delta C_{\mathrm{Au}}}{C_{\mathrm{Au}}}\right)^2 + \left(\frac{\Delta a_s}{a_s}\right)^2 + \left(\frac{\Delta I_{\gamma s}}{I_{\gamma s}}\right)^2 + \left(\frac{\Delta I_{\gamma \mathrm{Au}}}{I_{\gamma \mathrm{Au}}}\right)^2 \\ &+ \left(\frac{\Delta\varepsilon_s}{\varepsilon_s}\right)^2 + \left(\frac{\Delta\varepsilon_{\mathrm{Au}}}{\varepsilon_{\mathrm{Au}}}\right)^2 + 2\mathrm{Cov}(\varepsilon_s, \varepsilon_{\mathrm{Au}}) \\ &+ \left(\frac{\Delta f_s}{f_s}\right)^2 + \left(\frac{\Delta f_{\mathrm{Au}}}{f_{\mathrm{Au}}}\right)^2\end{aligned} \tag{A3}$$

where, $\mathrm{Cov}(\varepsilon_s, \varepsilon_{\mathrm{Au}})$ covariance between ε_s and $\varepsilon_{\mathrm{Au}}$., i.e.

$$\mathrm{Cov}(\varepsilon_s, \varepsilon_{\mathrm{Au}}) = \left(\frac{\Delta\varepsilon_s}{\varepsilon_s}\right) \mathrm{Corr}(\varepsilon_s, \varepsilon_{\mathrm{Au}}) \left(\frac{\Delta\varepsilon_{\mathrm{Au}}}{\varepsilon_{\mathrm{Au}}}\right) \tag{A4}$$

References

1. Handbook on photonuclear data for applications: Cross-sections and spectra (Final report of a co-ordinated research project 1996–1999), IAEA-TECDOC-1178.
2. Ikeda, Y.: Nuclear data relevant to accelerator driven system. J. Nucl. Sci. Technol. Suppl. **2**, 13 (2002).
3. Ganesan, S.: Nuclear data covariances in the Indian context-Progress, challenges, excitement and prospective. Nucl. Data Sheets **123**, 21 (2015).
4. Otuka, N., Dupont, E., Semkova, V., Pritychenko, B., Blokhin, A. I., Aikawa, M., Babykina, S., Bossant, M., Chen, G., Dunaeva, S., Forrest, R. A., Fukahori, T., Furutachi, N., Ganesan, S., Ge, Z., Gritzay, O. O., Herman, M., Hlavač, S., Katõ, K., Lalremruata, B., Lee, Y. O., Makinaga, A., Matsumoto, K., Mikhaylyukova, M., Pikulina, G., Pronyaev, V. G., Saxena, A., Schwerer, O., Simakov, S. P., Soppera, N., Suzuki, R., Takćs, S., Tao, X., Taova, S., Tárkányi, F., Varlamov, V. V., Wang, J., Yang, S. C., Zerkin, V., Zhuang, Y.: Experimental nuclear reaction data. Nucl. Data Sheets **120**, 272 (2014).

5. Deshpande, A., Araki, S., Dixit, T., Fukuda, M., Krishnan, R., Pethe, S., Sakaue, K., Terunuma, N., Urakawa, J., Vidwans, M., Washio, M.: S-band compact X-ray source with π/2 mode electron linac. Proceedings of Particle Accelerator Society Meeting 2009, JAEA, Tokai, Naka-gun, Ibaraki, Japan. 1177.
6. Punte, L. R. M., Lalremruata, B., Otuka, N., Suryanarayana, S. V., Iwamoto, Y., Pachuau, R., Satheesh, B., Thanga, H. H., Danu, L. S., Desai, V. V., Hlondo, L. R., Kailas, S., Ganesan, S., Nayak, B. K., Saxena, A.: Measurements of neutron capture cross section on ^{70}Zn at 0.96 and 1.69 MeV. Phys. Rev. C **95**, 024619 (2017).
7. Vidmar, T., Kanish, G., Vidmar, G.: Calculation of true coincidence summing corrections for extended sources with EFFTRAN. Appl. Radiat. Isot. **69**, 908 (2011).
8. Smith, D. L., Otuka, N.: Experimental nuclear reaction data uncertainties: Basic concepts and documentation. Nucl. Data Sheets **113**, 3006 (2012).
9. Mannhart W.: A small guide to generating covariances of experimental data. IAEA (NDS)-0588-Rev (2013).
10. Martin, M. J.: Nuclear data sheets for A=152. Nucl. Data Sheets **114**, 1497 (2013).
11. NuDat 2.7β, 2011, National Nuclear Data Center, Brookhaven National Laboratory, http://www.nndc.bnl.gov/.
12. Geraldo, L. P., Smith, D.: Covariance analysis and fitting of germanium gamma-ray detector efficiency calibration data. Nucl. Instru. Meth. Phys. Res. A **290**, 499 (1990).
13. Crasta, R., Naik, H., Suryanarayana, S. V., Prajapati, P. M., Jagadisan, K. C., Thakare, S. V., Ganesh, S., Nimje, V. T., Mittal, K. C., Goswami, A.: Photo-neutron cross-section of ^{100}Mo. J. Radioanal. Nucl. Chem. **290**, 367 (2011).
14. Qtool: calculation of reaction Q-values and threshold, http://cdfe.sinp.msu.ru/services/calc_thr/calc_thr.html.
15. Fasso, A., Ferrari, A., Ranft, J., Sala, P. R.: An update about FLUKA. In Proc. 2nd workshop on Simulating Accelerator Radiation Environment, SARE-2, CERN-Geneva. 9 (1995).
16. Fasso, A., Ferrari, A., Sala, P. R.: Designing of electron accelerator shielding with FLUKA. CERN internal report TIS-RP/IR/95-27m. 643 (1995).
17. Fasso, A., Ferrari, A., Sala, P. R.: Total giant resonance photonuclear cross sections for light nuclei: A database for the FLUKA Monte Carlo Transport Code. OECD-NEA 61 (1998).
18. Fasso, A., Ferrari, A., Sala, P. R.: Photonuclear reactions in FLUKA: cross sections and interaction models. AIP conf. Proc., **769**, 1303 (2005).
19. Bhat, M. R.: Nuclear data sheets for A= 57. Nucl Data Sheets **85**, 415 (1998).
20. Nesaraja, C. D., Geraedts, S. D., Singh, B.: Nuclear data sheets for A= 58. Nucl. Data Sheets **111**, 897 (2010).
21. Xiaolong, Huang.: Nuclear data sheets for A= 196. Nucl. Data Sheets. **108**, 1093 (2007)
22. Hara, K. Y., Harada, H., Kitatani, F., Goko, S., Hohara, S. Y., Kaihori, T., Makinaga, A., Utsunomiya, H., Toyokawa, H., Yamada, K.: Measurements of the ^{152}Sm(γ,n) cross section with laser-Compton scattering γ-rays and the photon difference method. J. Nucl. Sci. Technol. **44**, 938 (2007).
23. Kitatani, F., Harada, H., Goko, S., Utsunomiya, H., Akimune, H., Kaihori, T., Toyokawa, H., Yamada, K.: Measurement of the ^{80}Se (γ, n) cross section using laser-Compton scattering γ-rays. J. Nucl. Sci. Technol. **47**, 367 (2010).
24. Kitatani, F., Harada, H., Goko, S., Utsunomiya, H., Akimune, H., Toyokawa, H., Yamada, K.: Measurement of ^{76}Se and ^{78}Se (γ, n) cross sections. J. Nucl. Sci. Technol. **48**, 1017 (2011).
25. Itoh, O., Utsunomiya, H., Akimune, H., Kondo, T., Kamata, M., Yamagata, T., Toyokawa, H., Harada, H., Kitatani, F., Goko, S., Nair, C.: Photoneutron cross sections for Au revisited: measurements with laser Compton scattering γ-rays and data reduction by a least-squares method. J. Nucl. Sci. Technol. **48**, 834 (2011).
26. Plaisir, C., Hannachi, F., Gobet, F., Tarisien, M., Aléonard, M. M., Méot, V., Gosselin, G., Morel, P., Morillon, B.: Measurement of the ^{85}Rb (γ,n)^{84m}Rb cross-section in the energy range 10-19 MeV with bremsstrahlung photons. Eur. Phys. J. A. **48**, 1 (2012).
27. Otsuka, N., Lamremruta, B., Khandaker, M. U., Usman, A. R., Punte, L. R. M.: Uncertainty propagation in activation cross section measurements. Radiat. Phys. Chem. **140**, 502 (2017).
28. Sheela, Y. S., Naik, H., Prasad, K. M., Ganesan, S., Nair, N. S., Suryanarayana, S. V.: Covariance analysis of efficiency calibration of HPGe detector. Internal Report, No. MU/STATISTICS/DAE-BRNS/2017/1, 19-February-2017, DOI: 10.13140/RG.2.2.32025.21605.
29. Smith, D. L.: On the relationship between micro and macro correlations in nuclear measurement uncertainties. Nucl. Instru. Meth. Phys. Res. A **257**, 365 (1987).
30. Koning, A. J., Rochman, D., Kopecky, J., Sublet, J. C., Fleming, M., Bauge, E., Hilaire, S., Romain, P., Morillon, B., Duarte, H., Marck, S. C. V., Pomp, S., Sjostrand, H., Forrest, R., Henriksson, H., Cabellos, O., Goriely, S., Leppanen, J., Leeb, H., Lompen, A., Mills, R.: TENDL-2015: TALYS-based evaluated nuclear data library, available at https://tendl.web.psi.ch/tendl_2015/tendl2015.html.
31. Koning, A. J., Rochman, D.: Modern nuclear data evaluation with the TALYS code system. Nucl. Data Sheets **113**, 2841 (2012).
32. Kishida, N., Murata, T., Asami, T., Kosako, K., Maki, K., Harada, H., Lee, Y. O., Chang, J., Chiba, S., Fukahori, T. JENDL photonuclear data file. AIP Conf. Proc. **769**, 199 (2005).
33. Katz, L., Cameron, A. G. W.: The solution of x-ray activation curves for photonuclear cross sections. Can. J. Phys. **29**, 518 (1951).
34. Fultz, S. C., Alvarez, R. A., Berman, B. L., Meyer, P.: Photoneutron cross sections of ^{58}Ni and ^{60}Ni. Phys. Rev. C **10**, 608 (1974).
35. Goryachev, B. I., Ishkhanov, B. S., Kapitonov, I. M., Piskarev, I. M., Shevchenko, V. G., Shevchenko, O. P.: Photoneutron cross sections on nickel isotopes. Zh. Eksp. Teor. Fiz., Pis'ma Redaktsiyu **8**, 76 (1968).
36. Min, K., White, T. A.: Anomaly in the photodisintegration of ^{58}Ni and ^{60}Ni in the Giant-Dipole Resonance Region. Phys. Rev. Lett. **21**, 1200 (1968).
37. Ishkhanov, B. S., Kapitonov, I. M., Piskarev, I. M., Shevchenko, V. G. and Shevchenko, O. P.: Photoproton cross sections for nuclei with (1f-2p) shell. Yadern. Fiz. **11**, 485 (1970).
38. Owen, D. G.: Muirhead, E. G. Spicer, B. M.: Studies in the vibrational splitting of the giant dipole resonance:(II). ^{58}Ni and ^{60}Ni. Nucl. Phys. A **140**, 523 (1970).
39. Goryachev, B. I., Ishkhanov, B. S., Kapitonov, I. M., Piskarev, I. M., Shevchenko, V. G., Shevchenko, O. P.: Giant dipole resonance on Ni isotopes. Yadern. Fiz. **11**, 252 (1970).

40. Fultz, S. C., Bramblett, R. L., Caldwell, J. T., Hansen, N. E., Jupiter, C. P.: Photoneutron cross sections for ^{51}V and ^{59}Co. Phys. Rev. **128**, 2345 (1962).
41. Alvarez, R. A., Berman, B. L., Meyer, P., Jackson, H. E.: Photoneutron cross section of ^{55}Mn and ^{59}Co. Phys. Rev. C **20**, 128 (1979).
42. Baciu, G., Catana, D., Deberth, C., Iliescu, C. and Carstoiu, B.: Structure in the giant resonance of ^{59}Co. Nucl. Phys. A **167**, 177 (1971).
43. Goryachev, B. I., Ishkhanov, B. S., Kapitonov, I. M.: Structure of the photoneutron cross sections of ^{51}V, ^{52}Cr, ^{59}Co in region of the giant dipole resonance. Izv. Rossiiskoi Akademii Nauk, Ser.Fiz. **33**, 1736 (1969)
44. Baciu, G., Bonazzola, G. C., Minetti, B., Molino, C., Pasqualini, L., Piragino, G.: Photoneutron cross sections for Co, Ni, Cu and Ga. Nucl. Phys. **67**, 178 (1965).
45. Bazhanov, E. B., Komar, A. P., Kulikov, A. V.: Photoneutrons from Li^{6} and Co^{59}. Zh. Eksp. Teor. Fiz. **46**, 1497 (1964).